



Disorder and phase transitions in oxyfluoride $(\text{NH}_4)_3\text{Ta}(\text{O}_2)_2\text{F}_4$

I.N. Flerov^{a,b,*}, M.V. Gorev^{a,b}, V.D. Fokina^a, A.F. Bovina^a, E.V. Bogdanov^a, E.I. Pogoreltsev^a, N.M. Laptash^c

^a L.V. Kirensky Institute of Physics, Siberian Department of RAS, 660036 Krasnoyarsk, Russia

^b Siberian Federal University, 660074 Krasnoyarsk, Russia

^c Institute of Chemistry, Far Eastern Department of RAS, 690022 Vladivostok, Russia

ARTICLE INFO

Article history:

Received 24 March 2011

Received in revised form 11 May 2011

Accepted 13 May 2011

Available online 20 May 2011

Dedicated to our colleague and friend Dr. Alain Tressaud with sincere thanks for a long-standing fruitful collaboration and in recognition of his great contribution to Fluorine Chemistry.

Keywords:

Cubic oxyfluorides

Structural disorder

Phase transitions

Entropy

Permittivity

Pressure effect

ABSTRACT

Calorimetric, X-ray, dielectric and DTA under pressure measurements have been performed on oxyfluoride $(\text{NH}_4)_3\text{Ta}(\text{O}_2)_2\text{F}_4$. The succession of nonferroelectric phase transitions was found associated with the order-disorder processes. The comparative analysis tantalate with related niobate has revealed the important role of the central atom in the physical properties behavior, mechanism of structural distortions and barocaloric effect in oxyfluorides with the eight-coordinated anionic polyhedra.

© 2011 Elsevier B.V. All rights reserved.

1. Introduction

Recent years, the problem of structural disorder in materials has become increasingly popular among the chemists and physicists studying the relation between on the one hand thermodynamic and crystallographic stability of the crystal lattice and on the other transformations of different physical nature. Investigations of disordered systems in the vicinity of phase transition point are useful from fundamental and applied points of view because in such extreme conditions they show often a lot of interesting phenomena. One of them is associated with magneto- (MCE), electro- (ECE) and barocaloric (BCE) effects in solids. Materials exhibiting significant caloric efficiency are considered as the prominent refrigerants for solid state cooling devices which could be in competition with installations based on the vapor compression technology [1–3]. Caloric effects are characterized by the isothermal entropy change ΔS_{CE} or adiabatic temperature

change ΔT_{AD} on the application or withdrawal of the corresponding (magnetic H , electric E , mechanical stresses p) external field. Both effects are the most pronounced in materials exhibiting order-disorder phase transitions because the magnitudes of ΔS_{CE} as well as ΔT_{AD} depend strongly not only on the value of the external field, but also on the phase transition entropy ΔS [1]. Large susceptibility of phase transition to external field dT/dY ($Y: H, E, p$) also increases caloric efficiency of materials [1–4]. It is necessary to point out that there is not simple relation between the degree of disorder and the dT/dY value. For example this magnitude was found very large positive (+200 K/GPa) and negative (–28 K/GPa) in compounds $(\text{NH}_4)_3\text{MoO}_3\text{F}_3$ and $(\text{NH}_4)_2\text{KMoO}_3\text{F}_3$, respectively, undergoing order-disorder phase transitions characterized by close entropy values [5,6].

Up to the present, BCE in solids has not been studied so widely and intensively as ECE and MCE. However it is a very attractive property because of its generality for materials of any physical nature. Really, recently large barocaloric efficiency was observed in some materials undergoing martensitic, ferroelastic or ferroelectric phase transformations [3,7,8].

Materials with the perovskite-like crystal lattice show considerable promise to be disordered because of their great structural flexibility. This effect is the most pronounced in fluorides and

* Corresponding author. Present address: L.V. Kirensky Institute of Physics, Siberian Division, Russian Academy of Sciences, Krasnoyarsk 660036, Russia. Tel.: +7 391 249 45 07; fax: +7 391 2430 89 23.

E-mail address: flerov@iph.krasn.ru (I.N. Flerov).

oxyfluorides with the general chemical formulation $(A^+)_2 A' MeO_x F_{6-x}$ (x : 0, 1, 2, 3) having elpasolite–cryolite structure (sp. gr. $Fm\bar{3}m$, $Z = 4$). Experimental examinations have shown that a lot of these compounds undergo phase transitions associated with the ordering processes of some structural elements and followed by rather large entropy change $\Delta S \approx R \ln(6) - R \ln(16)$ [9–11]. Sixcoordinated structural units $[MeO_x F_{6-x}]$ are octahedral and pseudo-octahedral in fluorides and oxyfluorides, respectively. Cubic symmetry of oxyfluorides is due to two reasons. The former associates with the fluorine/oxygen ligands disorder in anion. The latter is resulted from relative orientations of the sixcoordinated units placed alongside each other leading to cancelling the dipole moments of separate pseudo-octahedra. Both types of disorder are the reason why oxyfluorides, in spite of inherently strongly polar anions, keep rather often nonferroelectric structure even in distorted phases realized as the result of phase transitions [11]. The entropy change associated with structural transformations in fluorides with ammonium cations exceeds the same in oxyfluorides. This is interesting and may be even strange because in the fluorine–oxygen compounds, besides orientational disorder of octahedra and tetrahedra, there is also a statistical disorder of oxygen–fluorine ligands. Nevertheless, because of the large susceptibility to hydrostatic pressure some oxyfluorides as well as fluorides with $[(NH_4)_3]$ and $[Rb_2K]$ cationic compositions exhibit comparable and significant in values BCE at rather low pressure [11].

Cubic structure $Fm\bar{3}m$ was found also in oxyfluorides with seven- and eightcoordinated anionic polyhedra containing peroxo-oxygen atoms [12–14]. To keep high symmetry, exotic structural units $[Me(O_2)_x F_{6-x}]$ (x : 1, 2; Me: Ti, Ta, Nb) as well as peroxo-oxygen group should be disordered [12–14].

Recently, it has been revealed that some of these compounds undergo structural phase transitions [15,16]. It is interesting that on the one hand the substitution of O atom by $[O_2]$ group leads to a significant decrease of phase transition entropy from $\Delta S \approx R \ln(9)$ in $(NH_4)_3 TiO_5$ to $\Delta S \approx R \ln(3)$ in $(NH_4)_3 Ti(O_2)F_5$. On the other hand among oxyfluorides with cryolite structure the largest value of entropy change $\Delta S \approx R \ln(16)$ was observed in $(NH_4)_3 Nb(O_2)_2 F_4$ containing two peroxo-oxygen atoms and undergoing the succession of nonferroelectric transformations [16]. One more intriguing result is that in related cryolite $(NH_4)_3 Ta(O_2)_2 F_4$ no phase transition has been observed by X-ray down to 120 K [12]. From our point of view it is rather strange because both oxyfluorides with the eightcoordinated anionic polyhedra are characterized by the same values of ionic radius of Me atoms and close unit cell parameters [13]. Moreover the same model of disorder in structure was suggested for ammonium niobate and tantalate.

Earlier we have met analogous situation studying the stability of cubic structure in $(NH_4)_3 MoO_3 F_3$ and $(NH_4)_2 KMoO_3 F_3$ [5,6]. Heat capacity measurements have shown that both oxyfluorides undergo order-disorder phase transitions. However, noticeable differences between the X-ray diffraction patterns of the initial and low-temperature phases were revealed in $(NH_4)_2 KMoO_3 F_3$ only. Structural changes in $(NH_4)_3 MoO_3 F_3$ were proved by temperature dependence of the unit cell parameter.

That is the reason why in this paper we continue the investigation of crystallographic stability of the cubic oxyfluorides with eightcoordinated polyhedra studying thermodynamic properties of $(NH_4)_3 Ta(O_2)_2 F_4$.

2. Synthesis, identification of the sample, and preliminary researches

Ammonium diperoxotetrafluorotantalate was prepared by dissolving Ta_2O_5 in concentrated (40%) hydrofluoric acid followed by adding H_2O_2 (30%) and ammonia solution (25%) to get $pH = 6$. Small crystals were formed under slow evaporation in air. The

composition of crystals was refined in accordance with the peroxo $(O_2)^{2-}$ group content determined by the permanganometry titrimetric method. The results revealed the 2 mass.% deficiency of $(O_2)^{2-}$ groups relative to stoichiometric composition $(NH_4)_3 Ta(O_2)_2 F_4$ (calc.: $(O_2)^{2-}$ 17.1). It means that some O^{2-} substituted for $(O_2)^{2-}$ groups like it was observed earlier by us in $(NH_4)_3 Nb(O_2)_2 F_4$ [16]. The real chemical composition of the compound corresponds to $(NH_4)_3 TaO_{0.2}(O_2)_{1.8}F_4$. Calc. for $(NH_4)_3 TaO_{0.2}(O_2)_{1.8}F_4$: $(O_2)^{2-}$ 15.5; found: $(O_2)^{2-}$ 15.1 ± 0.4 .

Structural characterization of $(NH_4)_3 Ta(O_2)_2 F_4$ was performed using X-ray powder diffractometry. The unit-cell constant has been refined at room temperature in the cubic space group: $a_0 = 0.9435(5)$ nm, and found to be in rather good agreement with the parameters determined in previous structural investigations – 0.9414(7) nm [12], 0.94512(4) nm [13]. There were not observed any additional phases in the sample.

The temperature stability of a cubic structure was studied by measurements carried out with a DSM-2 M differential scanning microcalorimeter (DSM) in the temperature range 120–270 K. The powdered compound was set in an aluminium sample holder. The experiments were performed in a helium atmosphere on several samples of mass 0.10–0.12 g. The heating and cooling rates were fixed at 8 K/min.

Fig. 1 depicts the experimental temperature dependence of the excess heat capacity ΔC_p for one of the samples. On cooling, one broad peak was observed with a maximum near 140 K. On the first heating, the heat capacity anomaly was detected as a sharp peak with a maximum at about $T_1 = 160$ K. On the next stages of thermal cycling a small shoulder-like anomaly has appeared on this peak at about $T_2 = 155$ K. The heat capacity behavior in cooling regime was always the same as on the first stage. The experimental results obtained have allowed us to suppose that $(NH_4)_3 Ta(O_2)_2 F_4$ after first cooling-heating cycle passes into thermodynamically stable state and undergoes two phase transitions of a strong first order characterized by rather different significant hysteresis in the temperatures of the heat capacity maximum and “shoulder”.

No noticeable differences between the X-ray diffraction patterns of the initial cubic and low-temperature phases were revealed. The presence of the structural changes associated with the phase transitions was identified from an anomalous behavior of the unit cell parameter between 150 K and 170 K (Fig. 2). It is interesting that in spite of large thermal hysteresis there is not strong change of the unit cell parameter at phase transitions point.

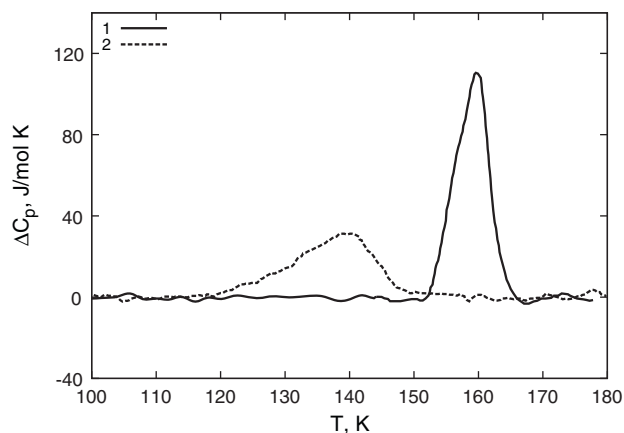


Fig. 1. Temperature dependence of the excess heat capacity of $(NH_4)_3 Ta(O_2)_2 F_4$ measured with DSM on cooling (2) and heating (1).

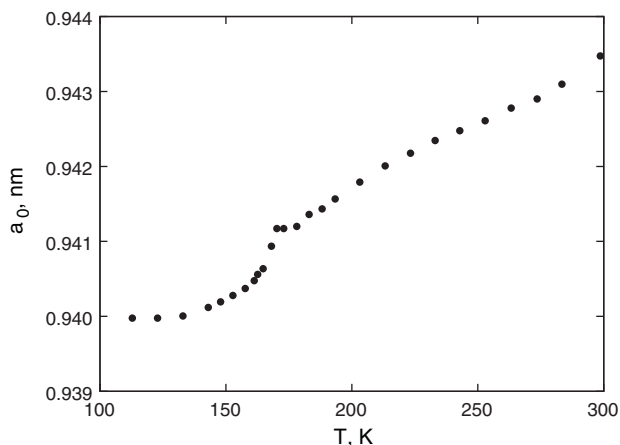


Fig. 2. Temperature dependence of the unit cell parameter of $(\text{NH}_4)_3\text{Ta}(\text{O}_2)_2\text{F}_4$ measured on heating.

3. Heat capacity measurements

Detailed heat capacity measurements on $(\text{NH}_4)_3\text{Ta}(\text{O}_2)_2\text{F}_4$ were performed with an adiabatic calorimeter. Powdered sample of a mass 1.532 g was set into an indium container sealed under helium atmosphere, which, in turn, was placed in accessories with a heater. The heat capacity of the accessories and indium cell was measured in individual experiment. Continuous ($dT/d\tau = 0.18\text{--}0.32\text{ K/min}$) and stepwise ($\Delta T = 1.8\text{--}2.0\text{ K}$) temperature changes were used to measure heat capacity in the temperature range 100–310 K.

The temperature dependence of the molar heat capacity obtained by adiabatic calorimeter is shown in Fig. 3a. It is necessary to point out that, as with DSM measurements, on the first heating from 140 to 180 K we have observed only one heat capacity anomaly at about 160 K (curve 1 in Fig. 3b). Next measurements in the same temperature range revealed two peculiar points $T_1 = 160.0 \pm 0.2\text{ K}$ and $T_2 = 155.0 \pm 0.2\text{ K}$ (curve 2 in Fig. 3b) which are in good agreement with temperatures of anomalies detected in DSM studies.

In Fig. 3a one can see also that, apart from the pronounced heat capacity anomalies corresponding to the phase transitions revealed in experiments with both calorimetric methods and in X-ray studies, the $C_p(T)$ behavior exhibits one more anomaly at $T_0 = 215.0 \pm 0.5\text{ K}$. Close inspection of X-ray data (Fig. 2) shows that near this temperature there is a small change in the $a_0(T)$ behavior.

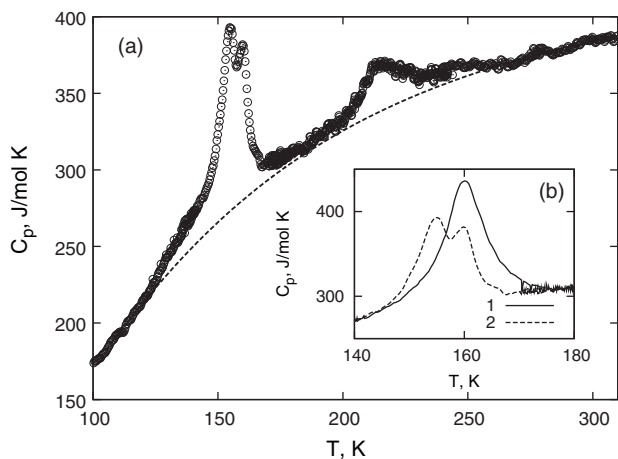


Fig. 3. Temperature dependence of the heat capacity for the $(\text{NH}_4)_3\text{Ta}(\text{O}_2)_2\text{F}_4$ oxyfluoride (dashed line indicates the lattice heat capacity) (a). Heat capacity in the region of T_1 and T_2 (1 and 2 are the first and following heating, respectively) (b).

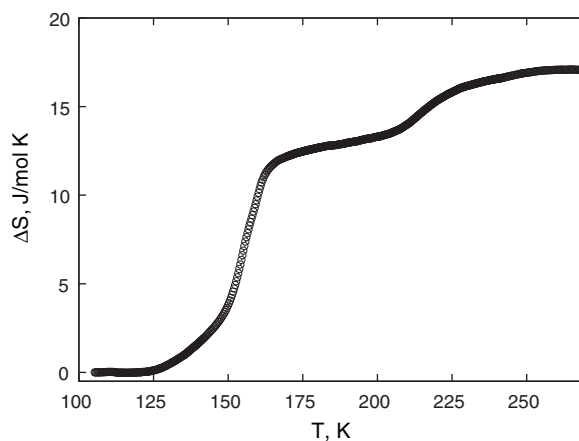


Fig. 4. Temperature dependence of entropy associated with phase transitions in $(\text{NH}_4)_3\text{Ta}(\text{O}_2)_2\text{F}_4$.

Both peculiarities suggest that, at the given temperature, there is a phase transition that could not be reliably revealed by the DSM method due to its lower sensitivity.

Separation of the lattice part, C_{lat} , and anomalous part, ΔC_p , of the heat capacity has been performed by fitting the experimental data taken far from the region of the phase transitions ($T < 125\text{ K}$ and $T > 260\text{ K}$) using Debye's and Einstein's functions, $C_{\text{lat}} = A_1 D(\Theta_D/T) + A_2 E(\Theta_E/T)$. The lattice contribution is shown as a dashed line in Fig. 3a. The average deviation of the experimental data from the smoothed curve does not exceed 0.75%. The relations between maximum values of excess heat capacity and C_{lat} are 0.1 (T_0), 0.37 (T_1) and 0.43 (T_2).

The enthalpy change associated with anomalous behavior of the heat capacity was determined by integration of the $\Delta C_p(T)$ function. Because of a small difference between T_1 and T_2 we could calculate only total values $\Delta H_1 + \Delta H_2 = 2000 \pm 150\text{ J/mol}$ and $\Delta H_0 = 840 \pm 60\text{ J/mol}$.

In the vicinity of T_1 points the heat capacity peaks are rather smeared and it was not possible to perform thermographic measurements to obtain information about hysteresis phenomena and latent heat. The temperature behavior of the excess entropy associated with the sequence of three phase transitions was studied by integrating the function $(\Delta C_p(T)/T)$ and is plotted in Fig. 4. The total entropy change $\Sigma \Delta S = 17.3 \pm 1.0\text{ J/mol K}$ consists of two parts: $\Delta S_1 + \Delta S_2 = 13.3 \pm 1.0\text{ J/mol K}$ and $\Delta S_0 = 4.0 \pm 1.0\text{ J/mol K}$.

4. Hydrostatic pressure effect. Dielectric measurements

The effect of hydrostatic pressure was studied on a sample which had been previously used for calorimetric measurements. Differential thermal analysis (DTA) was used to detect temperature associated with heat capacity anomalies. A small copper container filled with the powdered sample of $5 \times 10^{-2}\text{ cm}^3$ volume was glued onto one of two junctions of germanium–copper thermocouple. Quartz sample cemented to the other junction was used as a reference substance. The system thus mounted was placed inside the piston-and-cylinder type vessel associated with the multiplier. Pressure up to 0.75 GPa was generated using pentane as the pressure-transmitting medium. Temperature and pressure were measured with a copper-constantan thermocouple and manganin gauge with accuracies of about $\pm 0.3\text{ K}$, and $\pm 10^{-3}\text{ GPa}$, respectively.

The pressure-temperature phase diagram of $(\text{NH}_4)_3\text{Ta}(\text{O}_2)_2\text{F}_4$ was built from DTA experiments under pressure (Fig. 5).

To ensure the reliability of the results, the measurements were performed for both increasing and decreasing pressure cycles. There was detected only one DTA-anomaly associated in accor-

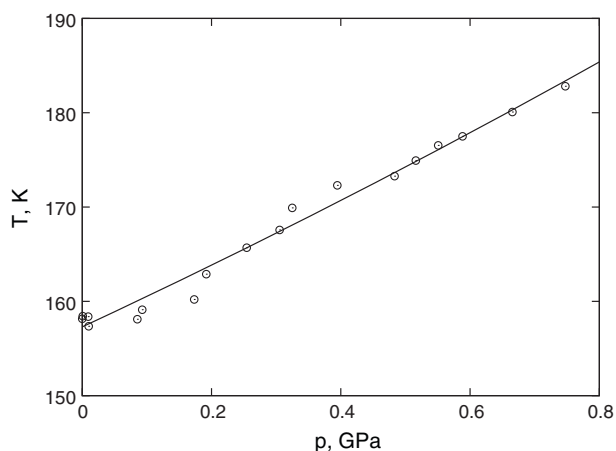


Fig. 5. The p - T phase diagram of $(\text{NH}_4)_3\text{Ta}(\text{O}_2)_2\text{F}_4$.

dance with temperature of the heat capacity maximum, from our point of view, with the phase transition at T_1 . The phase boundary can be described adequately with the equation of the type $T_1(p) = 157.3 + 31.9p + 4p^2$. Thus there is an almost linear increase of the phase transition temperature with pressure. No anomalies, which might be related to pressure-induced phase transitions, could be detected.

As was noted above, we did not succeed in preparing the $(\text{NH}_4)_3\text{Ta}(\text{O}_2)_2\text{F}_4$ oxyfluoride as bulk single crystal. Moreover, due to the low temperature of decomposition of ammonium compounds ceramic samples cannot be prepared using the traditional technique involving sintering at high temperatures. Therefore the permittivity was studied on the “quasi-ceramic” sample in the form of pressed pellet 8 mm in diameter and 2 mm in height prepared without heat treatment. Copper electrodes were deposited on a sample in a vacuum. Recently we have experimentally demonstrated that this way enables one to obtain reliable results [5,17].

The dielectric properties were measured using an E7-20 impedance meter at a frequency of 1 kHz on heating and cooling at a rate of ~ 0.6 K/min in the temperature range 120–270 K. The results of $\varepsilon(T)$ and $\text{tg}\delta(T)$ measurements are presented in Fig. 6.

The permittivity exhibits anomalous behavior represented as a step-wise increase from 10 to 12.5 in the temperature range 130–180 K (Fig. 6a) where there exists the excess heat capacity associated with phase transitions at T_1 and T_2 (Fig. 3a). At about in the same temperature region there was observed a peak of dielectric losses (Fig. 6b). In Fig. 6c one can see that the temperature hysteresis in dielectric measurements $\delta T \approx 5$ K is lower than in DSM measurements but it is still rather large. Strong increase of the $d\varepsilon/dT$ and $d(\text{tg}\delta)/dT$ derivatives above 210 K is most likely connected with dielectric losses in the “quasi-ceramic” sample prepared without heat treatment.

5. Discussion

Taking into account the same values of ionic radius of Nb and Ta atoms as well as the close structural parameters [13], one could expect the similar temperature behavior of $(\text{NH}_4)_3\text{Ta}(\text{O}_2)_2\text{F}_4$ and $(\text{NH}_4)_3\text{Nb}(\text{O}_2)_2\text{F}_4$ oxyfluorides containing in crystal lattice exotic anionic polyhedra. Really, the investigations performed in this paper revealed that the cubic structure stability in tantalate can be destroyed on cooling, as in the case of related niobate [16]. This result is in contradiction with that obtained in [12], where examination of X-ray powder diffraction patterns did not show any phase transition in $(\text{NH}_4)_3\text{Ta}(\text{O}_2)_2\text{F}_4$ at least down to 120 K. We have met the analogous situation in X-ray experiments too and

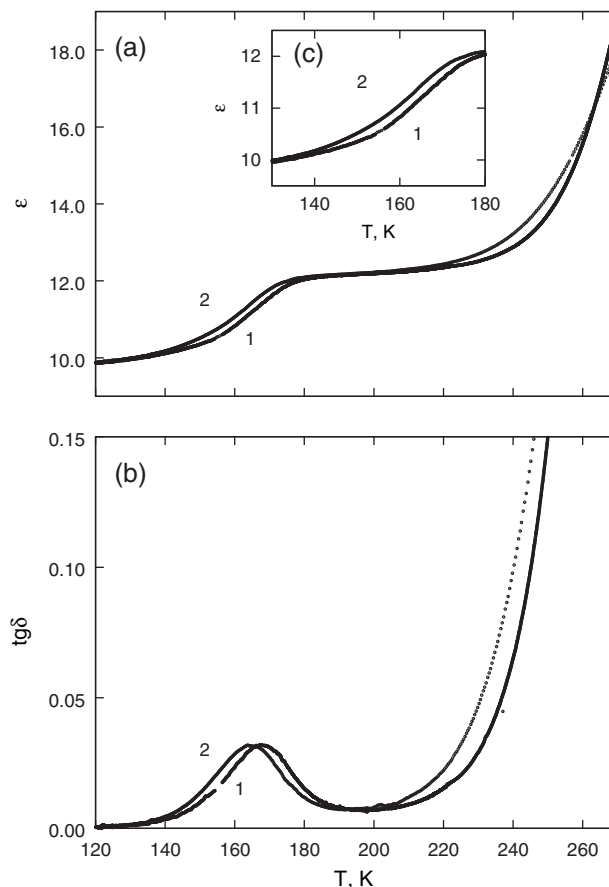


Fig. 6. Temperature dependences of the permittivity ε over a wide temperature range (a) and in the region of T_1 and T_2 (c), and the dielectric loss tangent $\text{tg}\delta$ (b) for $(\text{NH}_4)_3\text{Ta}(\text{O}_2)_2\text{F}_4$. 1 and 2 are the results on heating and cooling.

proved the structural changes in oxyfluoride under study by measuring temperature dependence of the unit cell parameter.

In Table 1 some experimental data for $(\text{NH}_4)_3\text{Ta}(\text{O}_2)_2\text{F}_4$ and $(\text{NH}_4)_3\text{Nb}(\text{O}_2)_2\text{F}_4$ are summarized. One can see that both oxyfluorides are characterized by rather close temperatures T_0 , T_1 , T_2 of heat capacity anomalies. Recall that, unlike tantalate, the value of ΔC_p at T_0 in niobate depends on the heating rate of the sample [16].

The common features of $(\text{NH}_4)_3\text{Ta}(\text{O}_2)_2\text{F}_4$ and $(\text{NH}_4)_3\text{Nb}(\text{O}_2)_2\text{F}_4$ are associated not only with an ability to lose on cooling the stability of the cubic phase. The mechanism, nature and order of structural transformations in tantalate and niobate are also the same. Really, rather large values of entropy change at all peculiar temperatures (Table 1) show that structural distortions are

Table 1
Thermodynamic parameters of the transitions in some oxyfluorides.

	$(\text{NH}_4)_3\text{Ta}(\text{O}_2)_2\text{F}_4$	$(\text{NH}_4)_3\text{Nb}(\text{O}_2)_2\text{F}_4$	$(\text{NH}_4)_3\text{MoO}_3\text{F}_3^a$
T_0 (K)	215	$\sim 240^a$	
T_1 (K)	160	193 ^a	297
T_2 (K)	155	187 ^a	205
$\Sigma\Delta S/R$	$\sim \ln 8$	$\sim \ln 48^a$	
$\Delta S_0/R$	$\sim \ln 1.6$	$\sim \ln 3^a$	
$(\Delta S_1 + \Delta S_2)/R$	$\sim \ln 5$	$\sim \ln 16^a$	$\ln 6$
dT_1/dp (K/GPa)	31.9	-57.4^a	202
dT_2/dp (K/GPa)		-44.4^a	46
p_{\min} (GPa)	1.5	0.5	0.07
$\Delta T_{\text{AD}}^{\max}$ (K)	6	-10	15
$\Delta S_{\text{BCE}}^{\max}/R$	-13	23	14

^a Data collected from [16] and [11] for $(\text{NH}_4)_3\text{Nb}(\text{O}_2)_2\text{F}_4$ and $(\text{NH}_4)_3\text{MoO}_3\text{F}_3$, respectively.

connected with some order–disorder processes. According to the thermodynamic theory of phase transitions [18], small stepwise change in the permittivity found in the temperature region, where heat capacity anomalies at T_1 and T_2 were observed, can be considered as associated with the first-order nonferroelectric transformations in both oxyfluorides. No anomalous behavior of $\varepsilon(T)$ has been observed at T_0 .

On the other hand, there is a series of individual peculiarities characteristic of both oxyfluorides. First of all, the absence of the structural reflection splitting in X-ray diffraction patterns of $(\text{NH}_4)_3\text{Ta}(\text{O}_2)_2\text{F}_4$ shows that the symmetry of its low temperature phases is other than that in $(\text{NH}_4)_3\text{Nb}(\text{O}_2)_2\text{F}_4$. One can think that this is one of the reasons why all ΔS values in niobate are nearly twice large as those for tantalate (Table 1). The ΔS_0 value for niobate is considered here as associated with the excess entropy above phase transitions region. At last, the susceptibility to hydrostatic pressure of oxyfluorides discussed is characterized by different sign of baric coefficients dT/dp (Table 1). In accordance with the Clausius–Clapeyron equation $dT/dp = \Delta V/\Delta S$, it means that on heating the unit cell volume of niobium and tantalum compounds decreases and increases, respectively, at phase transition point.

In [16] we have analysed the model of structural disorder in oxyfluorides with eightcoordinated polyhedra suggested in [12,13]. Taking into account a possibility of total ordering of $(\text{NH}_4)_3\text{Nb}(\text{O}_2)_2\text{F}_4$ structure as the result of phase transitions at T_1 and T_2 , a good agreement was found between experimentally determined entropy $\Delta S_1 + \Delta S_2$ (Table 1) and its calculated value $23.1 \text{ J/mol K} = R \ln(16)$. The latter value was obtained as the sum of entropies associated with the ordering of tetrahedra in the site *4b* ($R \ln(2)$) and eightcoordinated polyhedra ($R \ln(8)$) orientationally disordered on two and eight positions in a cubic phase.

Significant difference in the $\Delta S_1 + \Delta S_2$ values for oxyfluorides discussed let us to suppose that either $(\text{NH}_4)_3\text{Ta}(\text{O}_2)_2\text{F}_4$ undergoes another phase transition(s) below 100 K, or the structural elements of the this compound in the cubic phase remained disordered, although to a lesser extent compared to niobate.

No heat capacity anomalies, except for found in experiments with adiabatic calorimeter, have been observed by PPMs measurements on $(\text{NH}_4)_3\text{Ta}(\text{O}_2)_2\text{F}_4$ when cooling down to 2 K.

One can think that the second supposition is proved by the results of comparative structural study of $(\text{NH}_4)_3\text{Ta}(\text{O}_2)_2\text{F}_4$ and $(\text{NH}_4)_3\text{Nb}(\text{O}_2)_2\text{F}_4$ [13]. It was found that in both crystals the anisotropic vibrations are characteristic for N, F and O atoms.

However, the thermal parameters of all atoms even including central atoms Ta and Nb are significantly less in tantalate compared to niobate. In accordance with [19], the phase transition entropy depends on the degree of anharmonic vibrations of structural units playing active role in the mechanism of structural distortions. It is necessary to take in mind that to keep cubic structure, tetrahedra in 4b site should obligatory have at least two orientations. Thus the decrease of the $\Delta S_1 + \Delta S_2$ value in tantalum compound can be due to the decrease of anion disorder. To through light on the details of the phase transition mechanism one should get information on the structure of distorted phases in $(\text{NH}_4)_3\text{Ta}(\text{O}_2)_2\text{F}_4$ and $(\text{NH}_4)_3\text{Nb}(\text{O}_2)_2\text{F}_4$.

It is interesting to analyse the effect of the peculiarities in thermodynamic properties of both oxyfluorides on their barocaloric efficiency. The values of extensive ΔS_{BCE} and associated intensive $\Delta T_{\text{AD}} \text{ BCE}$

$$\Delta T_{\text{AD}} = -\left(\frac{T}{C_p}\right) \Delta S_{\text{BCE}} \quad (1)$$

were determined on the ground of approach used by us in [4,11]. Total entropy $S(T,p)$ of compounds undergoing phase transitions is the sum of the lattice S_{lat} and anomalous ΔS contributions. The baric coefficient dT/dp locates the position of $\Delta S(T)$ part on the $S(T)$ dependence

$$S(T, p) = S_{\text{lat}}(T) + \Delta S\left(T + \frac{dT}{dp} p\right). \quad (2)$$

The functions $S(T,p)$ for $(\text{NH}_4)_3\text{Ta}(\text{O}_2)_2\text{F}_4$ and $(\text{NH}_4)_3\text{Nb}(\text{O}_2)_2\text{F}_4$ were calculated on the ground of experimental results of the calorimetric and pressure measurements performed in the present paper and [16]. Fig. 7a and b shows that the behavior of the total entropies in both oxyfluorides is definitely different in accordance with different magnitudes of ΔS and dT/dp .

The value of ΔS_{BCE} was defined as the difference between total entropies under pressure and without pressure $\Delta S_{\text{BCE}}(T,p) = S(T,p) - S(T,0)$ at the same temperature. Intensive BCE was calculated from the condition of the entropy constancy at pressure change $S(T,0) = S(T + \Delta T_{\text{AD}},p)$. The temperature and pressure behavior of both BCE one can see in Fig. 8.

In line with the signs of baric coefficients, intensive as well as extensive effects in niobate and tantalate are characterized by different signs. Under pressure the former compound heats up and

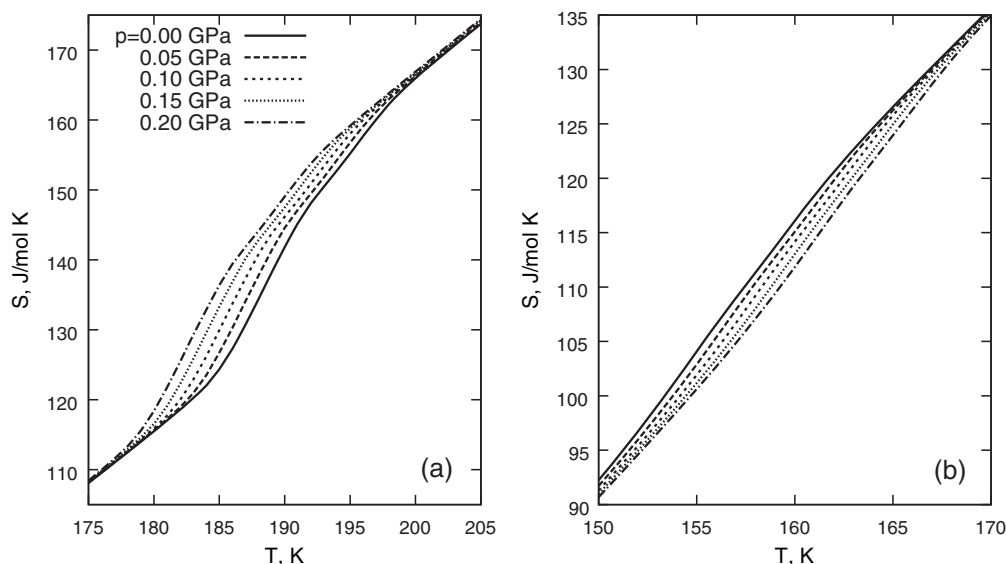


Fig. 7. Temperature dependences of the total entropy in $(\text{NH}_4)_3\text{Nb}(\text{O}_2)_2\text{F}_4$ (a) and $(\text{NH}_4)_3\text{Ta}(\text{O}_2)_2\text{F}_4$ (b).

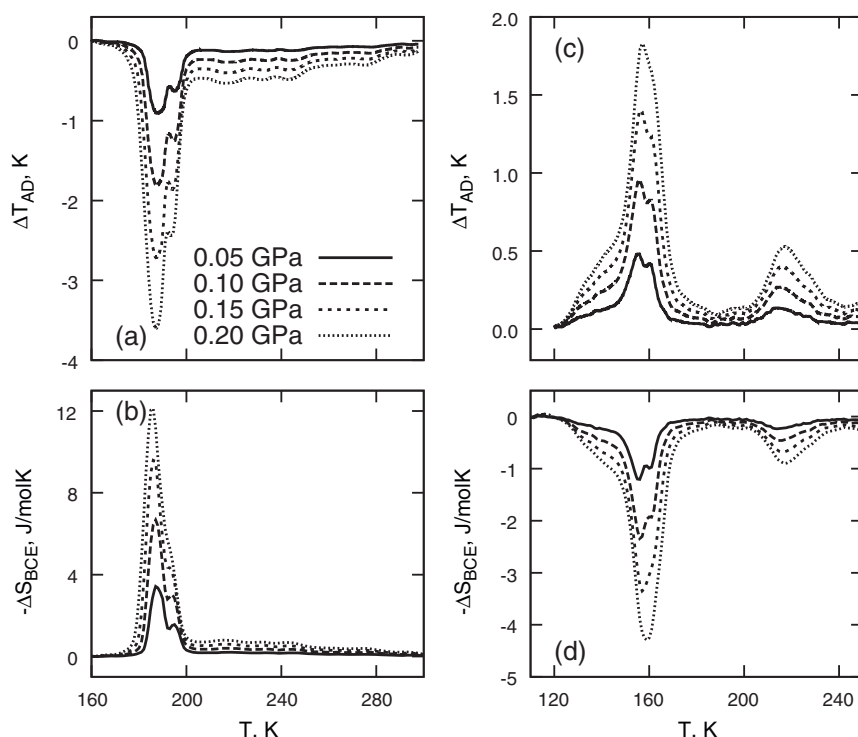


Fig. 8. Temperature dependences of intensive ΔT_{AD} and extensive ΔS_{BCE} barocaloric effects at various pressures in $(\text{NH}_4)_3\text{Nb}(\text{O}_2)_2\text{F}_4$ (a and b) and $(\text{NH}_4)_3\text{Ta}(\text{O}_2)_2\text{F}_4$ (c and d).

the latter cools down. It is seen also that at the same rather low pressure 0.2 GPa the $|\Delta T_{AD}|$ and $|\Delta S_{BCE}|$ values for $(\text{NH}_4)_3\text{Nb}(\text{O}_2)_2\text{F}_4$ are more than those for $(\text{NH}_4)_3\text{Ta}(\text{O}_2)_2\text{F}_4$ by factors of 2 and 3, respectively.

The maximum value of ΔS_{BCE}^{\max} is striving to the phase transition entropy ΔS . The ΔT_{AD}^{\max} value can be estimated as [11]

$$\Delta T_{AD}^{\max} = \Delta S \left(\frac{dS_{\text{lat}}}{dT} \right)^{-1} = \frac{\Delta S \cdot T}{C_{\text{lat}}} \quad (3)$$

The minimum values of pressure p_{\min} leading to the maximum magnitudes of the intensive and extensive BCE were determined using following equation [4,11]

$$p \geq \frac{T \cdot \Delta S}{C_{\text{lat}} \cdot dT/dp} \quad (4)$$

All barocaloric parameters discussed above are summarized in Table 1 and compared with those for oxyfluoride $(\text{NH}_4)_3\text{MoO}_3\text{F}_3$ with the sixcoordinated polyhedra [11]. One can see a great effect of baric coefficient on the p_{\min} and ΔT_{AD}^{\max} values. The pressure corresponding to maximum BCE in $(\text{NH}_4)_3\text{Nb}(\text{O}_2)_2\text{F}_4$ is less than that for $(\text{NH}_4)_3\text{Ta}(\text{O}_2)_2\text{F}_4$ by a factor of 3. On the other hand, in spite of rather small entropy of phase transition, molibdate is characterized by the largest ΔT_{AD}^{\max} value associated with very low pressure thanks to very large magnitude of dT/dp .

6. Concluding remarks

The study of thermodynamic properties has revealed that $(\text{NH}_4)_3\text{Ta}(\text{O}_2)_2\text{F}_4$ undergoes the succession of the order–disorder structural phase transitions of nonferroelectric nature. Comparison of the data obtained with those for related $(\text{NH}_4)_3\text{Nb}(\text{O}_2)_2\text{F}_4$ has shown a great effect of central atom on the peculiarities of phase transitions mechanism and barocaloric effects.

Acknowledgements

The authors are grateful to A.V. Kartashev for testing the heat capacity of the sample with PPMS.

This work was supported by the Council on Grants from the President of the Russian Federation for the Support of Leading Scientific Schools of the Russian Federation (NSH-4645.2010.2).

References

- [1] A.M. Tishin, Y.I. Spichkin, *The Magnetocaloric Effect and Its Applications in Series in Condensed Matter*, Institute of Physics, Bristol, Philadelphia, 2003.
- [2] E. Birks, M. Duncie, A. Sternberg, *Ferroelectrics* 400 (2010) 336–343.
- [3] L. Mañosa, D. González-Alonso, A. Planes, E. Bonnot, M. Barrio, J.-L. Tamarit, S. Aksoy, *M. Acet, Nat. Mater.* 9 (2010) 478–481.
- [4] M.V. Gorev, I.N. Flerov, E.V. Bogdanov, V.N. Voronov, N.M. Laptash, *Phys. Solid State* 52 (2010) 377–383.
- [5] I.N. Flerov, V.D. Fokina, A.F. Bovina, E.V. Bogdanov, M.S. Molokeev, A.G. Kocharova, E.I. Pogorel'tsev, N.M. Laptash, *Phys. Solid State* 50 (2008) 515–524.
- [6] I.N. Flerov, M.V. Gorev, V.D. Fokina, A.F. Bovina, M.S. Molokeev, E.I. Pogorel'tsev, N.M. Laptash, *Phys. Solid State* 49 (2007) 141–147.
- [7] M.V. Gorev, E.V. Bogdanov, I.N. Flerov, V.N. Voronov, N.M. Laptash, *Ferroelectrics* 397 (2010) 76–80.
- [8] E.A. Mikhaleva, I.N. Flerov, V.S. Bondarev, M.V. Gorev, A.D. Vasiliev, T.N. Davydova, *Phys. Solid State* 53 (2011) 510–517.
- [9] I.N. Flerov, M.V. Gorev, K.S. Aleksandrov, A. Tressaud, J. Grannec, M. Couzi, *Mater. Sci. Eng. R24* (1998) 81–150.
- [10] I.N. Flerov, M.V. Gorev, K.S. Aleksandrov, A. Tressaud, V.D. Fokina, *Crystallogr. Rep.* 49 (2004) 100–107.
- [11] I.N. Flerov, M.V. Gorev, A. Tressaud, N.M. Laptash, *Crystallogr. Rep.* 56 (2011) 9–17.
- [12] R. Schmidt, G. Pausewang, W. Massa, *Z. Anorg. Allg. Chem.* 488 (1982) 108–120.
- [13] Ž. Ružič-Toroš, D. Kojić-Prodić, *Inorg. Chim. Acta* 86 (1984) 205–208.
- [14] D. Bayot, M. Devillers, D. Peeters, *Eur. J. Inorg. Chem.* (2005) 4118–4123.
- [15] I.N. Flerov, M.V. Gorev, V.D. Fokina, M.S. Molokeev, A.D. Vasil'ev, A.F. Bovina, N.M. Laptash, *Phys. Solid State* 48 (2006) 1559–1567.
- [16] V.D. Fokina, A.F. Bovina, E.V. Bogdanov, E.I. Pogorel'tsev, N.M. Laptash, M.V. Gorev, I.N. Flerov, *Phys. Solid State*, accepted.
- [17] E. Pogorel'tsev, I. Flerov, N. Laptash, *Ferroelectrics* 401 (2010) 207–210.
- [18] B.A. Strukov, A.P. Levanyuk, *Ferroelectric Phenomena in Crystals*, Physical Foundations, Springer, Berlin, 1998.
- [19] V.G. Vaks, *Vvedenie v mikroskopicheskuyu teoriyu cegnetoelektrikov*, Nauka, Moscow, 1973 (in Russian).